






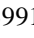





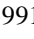
Generalizable SoH Estimation for Li-ion Batteries via Identity Embeddings: A CNN/GRU/LSTM Comparative Study





Estimación generalizable del SoH para baterías Li-ion mediante Identity Embeddings: estudio comparativo CNN/GRU/LSTM

Medina-Martínez, Sergio Iván^{*a}, Juárez-Toledo, Carlos^b, Martínez-Carrillo, Irma^c and Hernández-Epigmenio, Miguel Angel^d

^a  Universidad Autónoma del Estado de México - Unidad Académica Profesional Tianguistenco •  LBY-0431-2024 •  0000-0002-6094-2177 •  1083727

^b  Universidad Autónoma del Estado de México - Unidad Académica Profesional Tianguistenco •  C-1368-2016 •  0000-0002-7440-3246 •  39912

^c  Universidad Autónoma del Estado de México - Unidad Académica Profesional Tianguistenco •  B-9264-2016 •  0000-0002-7952-4418 •  39914

^d  Universidad Autónoma del Estado de México - Centro Universitario UAEM Tianguistenco •  F-9514-2018 •  0000-0002-4902-6936 •  786771

Clasificación SECIHTI:

Area: Engineering

Field: Technological sciences

Discipline: Computer technology

Subdiscipline: Artificial intelligence

 <https://doi.org/10.35429/JOCT.2025.9.22.4.1.9>

History of the article:

Received: August 30, 2025

Accepted: December 02, 2025

*  []

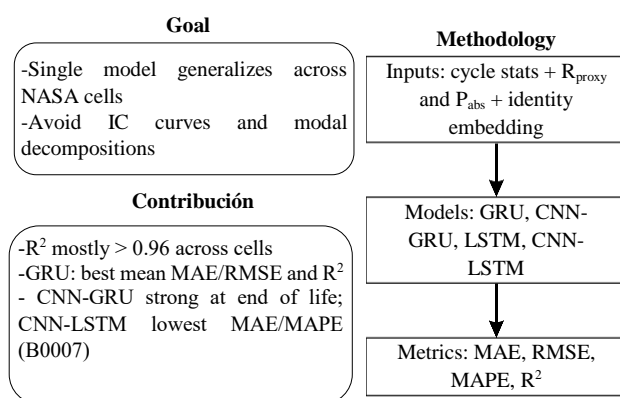


Abstract

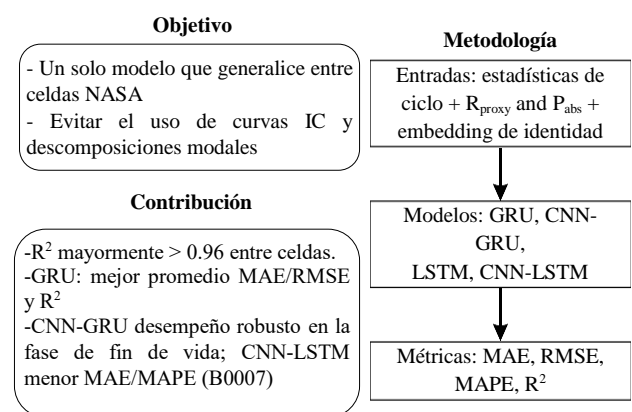
A generalizable deep learning method for Li-ion battery SoH (State of Health) is proposed. An identity embedding conditions the model to the degradation of each cell; physics-guided features R_{proxy} and P_{abs} complement cycle statistics. We compare GRU, CNN-GRU, LSTM, and CNN-LSTM on NASA cells B0005–B0007/B0018. Hyperparameters are tuned with validation; MAE, RMSE, MAPE, and R^2 are reported on held-out tests. All architectures track the SoH with high fidelity (R^2 mostly >0.96). On average, GRU achieves the lowest MAE/RMSE and the highest R^2 ; CNN-GRU handles end-of-life transitions well; CNN-LSTM obtains the lowest MAE/MAPE on B0007.

Resumen

Se propone un método de aprendizaje profundo generalizable para el SoH de baterías Li-ion. Un identity embedding condiciona el modelo a la degradación de cada celda; rasgos guiados por física R_{proxy} and P_{abs} complementan estadísticas de ciclo. Comparamos GRU, CNN-GRU, LSTM y CNN-LSTM en las celdas NASA B0005–B0007/B0018. Los hiperparámetros se ajustan con validación; MAE, RMSE, MAPE y R^2 se reportan en pruebas retenidas. Todas las arquitecturas siguen el SoH con alta fidelidad (R^2 mayormente >0.96). En promedio, GRU logra el menor MAE/RMSE y el mayor R^2 ; CNN-GRU presenta desempeño robusto en la fase de fin de vida (EoL), capturando transiciones rápidas con bajo error.; CNN-LSTM obtiene el menor MAE/MAPE en B0007.



Deep learning, Identity embedding, State of Health



Aprendizaje profundo, Incorporación de identidad, Estado de Salud

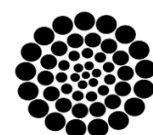
Area: Promotion of frontier research and basic science in all fields of knowledge

Citation: Medina-Martínez, Sergio Iván, Juárez-Toledo, Carlos, Martínez-Carrillo, Irma and Hernández-Epigmenio, Miguel Angel. [2025]. Generalizable SoH Estimation for Li-ion Batteries via Identity Embeddings: A CNN/GRU/LSTM Comparative Study. Journal of Computational Technologies. 9[22]1-9: e4922109.



ISSN: 2523-6814 / © 2009 The Author[s]. Published by ECORFAN-Mexico, S.C. for its Holding Taiwan on behalf of Journal of Computational Technologies. This is an open access article under the CC BY-NC-ND license [<http://creativecommons.org/licenses/by-nc-nd/4.0/>]

Peer review under the responsibility of the Scientific Committee MARVID[®] in the contribution to the scientific, technological and innovation Peer Review Process through the training of Human Resources for continuity in the Critical Analysis of International Research.



RENIECT
Registro Nacional de Instituciones y
Empresas Científicas y Tecnológicas

1702902 SECIHTI

Introduction

One of the main applications of lithium-ion batteries (LIBs) is in electric vehicles (EVs), driven by the need to reduce dependence on fossil fuels and mitigate climate change. LIBs are characterized by their high energy density (120–220 Wh/kg), long cycle life (~2000 cycles), and low maintenance requirements. Nevertheless, significant limitations remain, including the high cost—which accounts for approximately 30% of the total cost of an EV—and the risk of overheating.

Among the most widely used LIB chemistries are lithium iron phosphate (LFP, LiFePO_4), known for their safety and low cost but lower energy density; lithium nickel cobalt manganese oxide (NCM, LiNiMnCoO_2), which provide a balance between safety, energy density, and lifespan; and lithium nickel cobalt aluminum oxide (NCA, LiNiCoAlO_2), which offer high energy density suitable for long-range EVs but are more thermally unstable (Ralls *et al.*, 2023; Shen *et al.*, 2018).

Given these challenges, safety is a critical factor, making the implementation of battery management systems (BMSs) indispensable. These systems not only prevent short circuits and overheating but also enable the estimation of key parameters such as the state of charge (SoC), state of health (SoH), and remaining useful life (RUL).

Current trends in BMS development highlight the integration of artificial intelligence (AI) and cloud computing, which improve prediction accuracy and reduce the risk of failures. In this context, the present work focuses on the implementation of AI-based approaches for the prediction of the SoH of LIBs (Tran *et al.*, 2022; Yang *et al.*, 2021).

The SoH of a battery is inherently a sequential process, so recurrent neural networks (RNNs) are well-suited for their estimation. Among them, the long short-term memory (LSTM) network has become one of the most widely adopted due to its ability to capture long-term temporal dependencies. Moreover, these architectures can be combined with other types of networks, such as convolutional neural networks (CNNs), to enhance feature extraction.

In this regard, an improved model for SoH estimation of LIBs, based on a CNN-LSTM architecture with skip connections, integrates the incremental capacity (IC) curve as an input feature and employs a feature selection algorithm to eliminate redundant information, thereby reducing computational complexity; the model was validated on the NASA and Oxford datasets, achieving superior accuracy (Root Mean Square Error (RMSE) < 0.004) and greater robustness compared to previous architectures, thus demonstrating its ability to generalize across different cells within each dataset (Xu *et al.*, 2023)

Other studies have focused on improving input-feature quality and guiding LSTM networks to prioritize the most informative portions of the historical sequence rather than weighting all time steps equally, while also incorporating stochastic methods to enhance robustness. For example, an enhanced LSTM-based framework for LIB SoH estimation couples variational mode decomposition (VMD)—to separate long-term degradation trends from local fluctuations—with an LSTM augmented by a self-attention (SA-LSTM) mechanism to capture long-range temporal dependencies, while a particle filter (PF) models the residual (trend) component; trained and validated on the NASA Ames repository with inputs including current, voltage, temperature, SoC, and derived features, this approach outperformed Bi-LSTM and support vector regression (SVR) baselines, achieving RMSE values between 0.84 and 1.4 across cells (Ravi *et al.*, 2022)

Alternatively, several studies employ gated recurrent unit (GRU) networks as a variant of RNNs owing to their lower parametric complexity relative to LSTM and consequently shorter training times. These networks can also be integrated with other architectures; for example, an end-to-end CNN-GRU architecture for the joint estimation of SoH and RUL uses a 1D CNN as an automatic feature extractor, a GRU for long-range temporal dependencies, and a fully connected layer for outputs; meta-optimization via the artificial lemming algorithm (ALA) tunes key hyperparameters, and reported performance shows Mean Absolute Error (MAE) in the range $(2.5\text{--}3.9) \times 10^{-3}$ (Yu & Pan, 2025).

Additionally, for the NASA subset (batteries B0005, B0006, B0007, B0018), a three-stage CS–VMD–GRU pipeline—(1) decomposing the capacity time series with VMD and automatically optimizing key hyperparameters (number of modes and penalty) via cuckoo search (CS), (2) training one GRU per intrinsic mode function (IMF) and reconstructing capacity after normalization, and (3) converting reconstructed capacity into RUL using an end-of-life (EOL) threshold of 70%—achieves maximum RMSE $\leq 3\%$, maximum MAE $\leq 2\%$, with mean RMSE = 0.0142 and mean MAE = 0.0112 (Ding *et al.*, 2022).

Finally, using NASA data (batteries B0005, B0006, B0007, B0018, and B0036) with preprocessing (cleaning, Pearson-correlation-based feature selection, and normalization) and a 90/10 train/test split, a centralized comparison of 1D-CNN, CNN+LSTM, and CNN+GRU shows 1D-CNN as the most consistent overall, while recurrent variants capture temporal dependencies and can excel on specific batteries (e.g., GRU on B0005). A federated learning (FL) scheme with five clients enables training without sharing raw data, balancing privacy and performance, though with higher test errors than centralized training (e.g., RMSE ≈ 0.666 , MAPE ≈ 0.980) (Alharbi *et al.*, 2025).

In this study, a novel deep learning method for the precise estimation of SoH in LIBs is proposed. The central innovation is a battery-identity embedding that transforms a discrete identifier for each unit into a learnable vector representation, conditioning the model on the unique degradation characteristics of each battery and enabling a single, unified model to generalize across heterogeneous devices. Furthermore, a proxy calculation for internal resistance proxy (R_{proxy}) and an integrated absolute-power proxy (P_{abs}) are introduced. Experimental results on the NASA prognostic dataset show high predictive accuracy without needing IC analysis or VMD-type decompositions.

Methodology

For SoH estimation, we use the LIB aging dataset provided by the NASA Prognostics Center of Excellence (NASA PCoE), a standard in the field due to strictly controlled experimental conditions (Saha & Goebel, 2007).

For this study, data from B0005, B0006, B0007, and B0018 were selected to develop a generalized model for different degradation profiles. The batteries were subjected to charge/discharge profiles at 24 °C. Charging used constant current (CC) at 1.5 A to 4.2 V, followed by constant voltage (CV) to 20 mA. Discharge was carried out at 2 A to 2.7 V (B0005), 2.5 V (B0006), and 2.2 V (B0007); B0018 was discharged at 4 A to 2.5 V. Experiments ended at EOL defined as a 30% reduction in rated capacity (2 Ah \rightarrow 1.4 Ah) (Medina-Martínez *et al.*, 2024).

The SoH is defined as the ratio between the current capacity and the initial capacity (Eq. [1]). Base features include cycle duration and average voltage, current, and temperature. Additionally, two features were engineered to capture physical degradation: an internal-resistance proxy R_{proxy} , computed from integrated voltage and absolute current (Eq. [2]), and an integrated absolute-power proxy P_{abs} to quantify cycle energy (Eq. [3]); P_{abs} is expected to decrease with aging due to capacity fade and increased internal resistance, with clear decay patterns (Figures 1 and 2).

$$\text{SoH} = \frac{\text{Capacity}_{\text{current}}}{\text{Capacity}_{\text{initial}}} \quad [1]$$

$$R_{\text{proxy}} = \frac{\int V(t)dt}{\int |I(t)dt|} \quad [2]$$

$$P_{\text{abs}} = \int V(t)dt \times \int |I(t)dt| \quad [3]$$

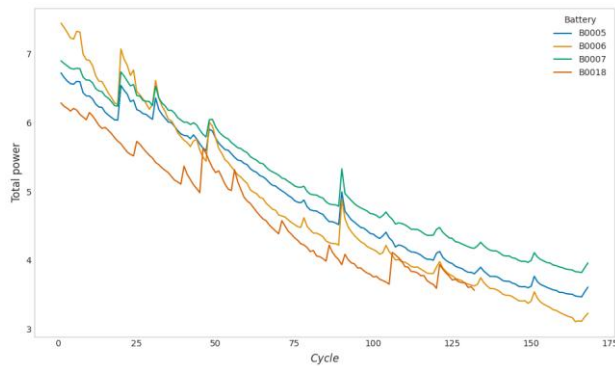
Box 1



Figure 1

Resistance proxy trend per Cycle in Four LIBs

Source: Own elaboration

Box 2**Figure 2**

Total Power vs. Cycle in Four LIBs

Source: Own elaboration

For SoH prediction, four deep neural network architectures were evaluated, designed to effectively capture temporal dependencies and local patterns in the battery cycle data. These architectures are divided into two categories: base recurrent models (GRU and LSTM) and hybrid (CNN+GRU and CNN+LSTM).

GRU and LSTM are advanced recurrent architectures, designed to overcome the limitations of traditional RNNs, such as the vanishing gradient problem in long sequences. Their main strength lies in their gating mechanisms, which allow them to learn what information to retain or discard over time. While LSTM uses a three-gate mechanism (input, forget, and output) and an explicit memory cell, the GRU features a simplified architecture with two gates (update and reset), which generally results in faster training with comparable performance, making it more suitable for embedded system implementations (Kong *et al.*, 2025.; Luo *et al.*, 2022).

To better capture local patterns, hybrid models place a CNN block before the recurrent layers: the CNN extracts short-range features across battery signals, while the recurrent module models their temporal evolution over cycles (Eleftheriadis *et al.*, 2024; Peng *et al.*, 2023). To generalize a single model across multiple batteries with heterogeneous degradation profiles, the battery's identity is integrated as a learnable input feature. This approach is framed within the paradigm of Representation Learning, which aims to acquire significant latent features in a compact, low-dimensional space (Chen *et al.*, 2025; Cheng, 2025).

Unlike the positional embeddings used in Transformer architectures to encode sequence order, our identity embedding captures the static and unique characteristics of each battery. The process is as follows:

- Numerical Labeling: Each unique battery identifier (e.g., 'B0005') is assigned an integer numerical label.
- Embedding Layer: This label is fed into a Keras Embedding layer. This layer maps the categorical identifier to a dense, learnable vector in a latent space of a fixed dimension.
- Identity Vector: During training, the model adjusts this vector to act as a "signature" that captures the intrinsic degradation characteristics of that specific battery.
- Concatenation: This identity vector is then concatenated with the time-series data at each step, allowing a single, unified model to learn both the general degradation patterns and the nuances of each unit.

Finally, figure 3 visually summarizes the entire methodology, from raw-data processing to final prediction. It depicts five key preprocessing stages that produce training, validation, and test sets (80%, 10%, 10%). The model architecture is then detailed: the cycle sequence and the battery identity (encoded via an Embedding layer) enter as parallel inputs. For both base and hybrid models, the data flow is shown—optionally passing the sequence through a CNN block, concatenating it with the identity vector, and finally processing it with a recurrent block (GRU or LSTM)

Box 3

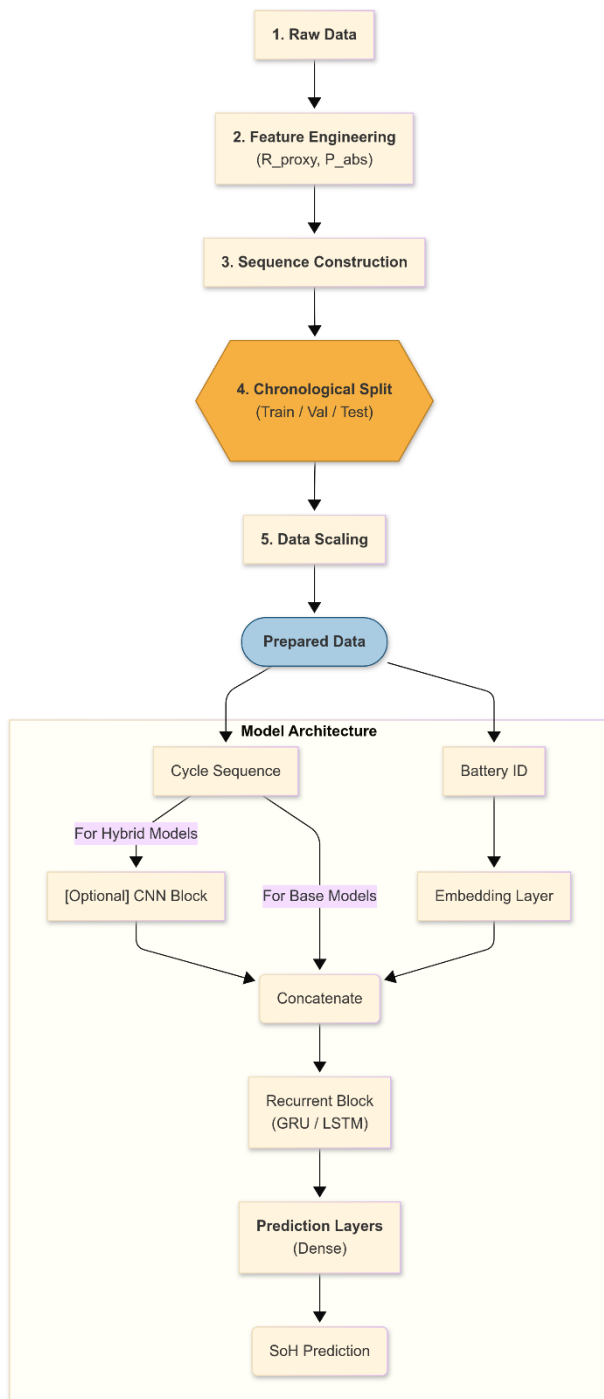


Figure 3
Sequence Construction and Hybrid Architecture for SoH Prediction

Source: Own elaboration

Results

For each of the four deep architectures (GRU, CNN-GRU, LSTM, CNN-LSTM), we performed hyperparameter tuning to optimize predictive performance. Through an experimental process, the values that minimized the validation error were selected. The final hyperparameters used for training each model are summarized in Table 1.

Box 4

	GRU	CNN + GRU	LSTM	CNN + LSTM
Sequence	15	5	5	5
Batch	8	64	8	64
LR	5×10^{-4}	1×10^{-3}	5×10^{-4}	5×10^{-4}
Units	128	128	256	128
Filters	NA	64	NA	64
Kernel	NA	5	NA	3

Table 1
Final hyperparameters used for each deep model
Source: Own Elaboration

Using these configurations, we evaluated predictive performance on the test sets with MAE, RMSE, MAPE, R^2 . As shown in Table 2, all models captured the battery degradation trend with high fidelity R^2 values are mostly above 0.96 (one case at 0.9593) and low absolute errors across batteries.

Box 5

	MAE			
	GRU	CNN-GRU	LSTM	CNN-LSTM
B0005	0.0043	0.0081	0.0170	0.0065
B0006	0.0140	0.0129	0.0158	0.0152
B0007	0.0058	0.0073	0.0057	0.0054
B0018	0.0034	0.0110	0.0083	0.0080
MAPE				
B0005	0.0050	0.0097	0.0203	0.0078
B0006	0.0196	0.0173	0.0216	0.0213
B0007	0.0066	0.0084	0.0066	0.0062
B0018	0.0040	0.013	0.0099	0.0095
RMSE				
B0005	0.0054	0.0104	0.0191	0.0090
B0006	0.0176	0.0162	0.0192	0.0200
B0007	0.0070	0.0094	0.0076	0.0078
B0018	0.0043	0.0161	0.0110	0.0125
R^2				
B0005	0.9968	0.9892	0.9641	0.9918
B0006	0.9742	0.9814	0.9738	0.9716
B0007	0.9923	0.9872	0.9915	0.9910
B0018	0.9962	0.9593	0.9807	0.9754

Table 2
Comparison of error metrics and coefficient of determination by Model and Battery
Source: Own Elaboration

Finally, as shown in Figs. 4–7, it is confirmed that all architectures exhibit strong generalization to SoH degradation, with small cycle-level errors. GRU provides the best balance between responsiveness and stability with tight, well-centered residuals and minimal lag resulting in the lowest average MAE/RMSE and the highest average R^2 across batteries. CNN-GRU handles rapid end-of-life transitions particularly well (notably for B0006).

CNN-LSTM yields the smoothest trajectories and achieves the lowest MAE/MAPE for B0007, albeit with slight over-smoothing in sharp variations. In contrast, plain LSTM follows the trend but is outperformed by the other configurations.

- B0005: GRU achieves the best MAE/RMSE and highest R^2 .
- B0006: CNN-GRU achieves the best MAE/RMSE and highest R^2 .
- B0007: CNN-LSTM has the lowest MAE and MAPE; GRU attains the lowest RMSE and the highest R^2 .
- B0018: GRU attains the lowest MAE/RMSE and the highest R^2 .

Compared with CNN-LSTM approaches that rely on incremental-capacity inputs and feature-selection stages (e.g., Xu *et al.*, 2023), our study employs an identity embedding and simple physics-informed features (R_{proxy} , P_{abs}) to enable a single end-to-end model without IC preprocessing or modal decompositions. Relative to CS-VMD-GRU pipelines (Ding *et al.*, 2022), we avoid variational mode decomposition and per-IMF training, thereby reducing modeling complexity and pre-analysis overhead.

In contrast to Alharbi *et al.* (2025), who reported the most consistent centralized performance for 1D-CNN across a broader NASA subset (including B0036) under a 90/10 split, our experiments on B0005, B0006, B0007, B0018 indicate that GRU achieves the best average MAE, RMSE and R^2 , CNN-GRU excels on rapid end-of-life transitions (B0006), and CNN-LSTM attains the lowest MAE/MAPE on B0007.

Finally, unlike SA-LSTM + particle-filter hybrids (Ravi *et al.*, 2022), our models do not incorporate explicit probabilistic filtering or attention mechanisms, prioritizing architectural simplicity and ease of deployment.

Box 6

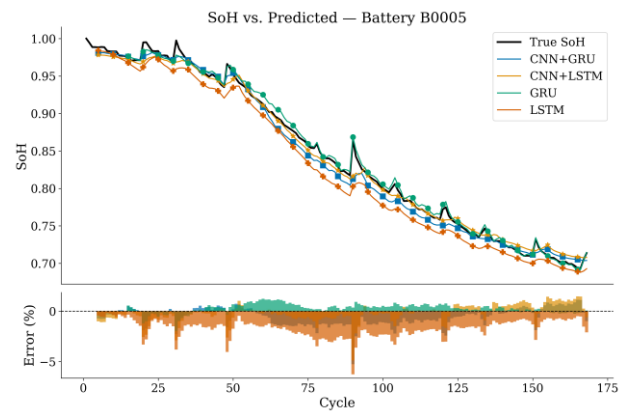


Figure 4

SoH Prediction vs. Ground Truth-Battery B0005

Source: Own Elaboration

Box 7

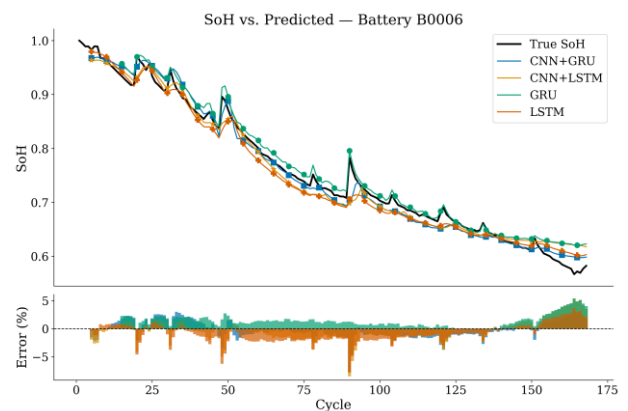


Figure 5

SoH Prediction vs. Ground Truth-Battery B0006

Source: Own Elaboration

Box 8

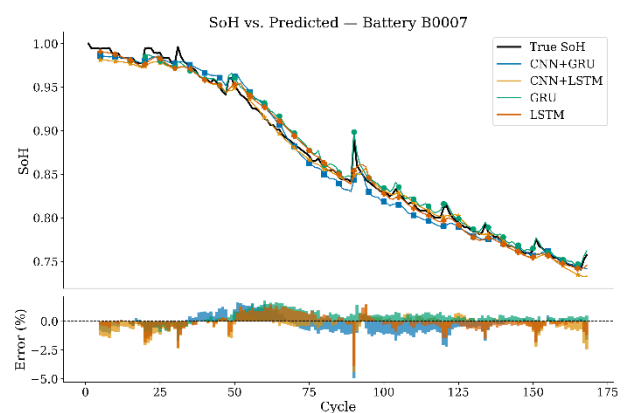


Figure 6

SoH Prediction vs. Ground Truth-Battery B0007

Source: Own Elaboration

Box 9

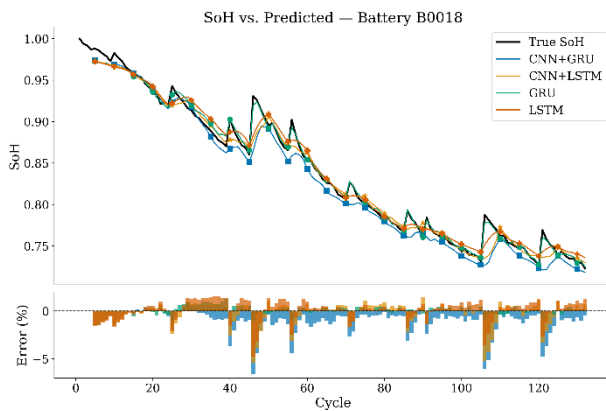


Figure 7

SoH Prediction vs. Ground Truth-Battery B0018

Source: Own Elaboration

Conclusions

We introduced a unified deep-learning approach for SoH estimation that combines battery-identity embedding with physics-informed features (R_{proxy} , P_{abs}). On NASA cells B0005/B0006/B0007/B0018, all architecture generalizes well; on average, GRU attains the lowest MAE/RMSE and highest R^2 . GRU's strong average accuracy, coupled with its lower parametric complexity, makes it an attractive choice for embedded BMS deployments. CNN-GRU excels under rapid end-of-life transitions, and CNN-LSTM achieves the best MAE/MAPE on B0007.

Limitations & future work:

- Validate across chemistries, temperatures, and real drive cycles (beyond NASA, fixed conditions).
- Add uncertainty quantification and calibration for deployment.
- Explore domain adaptation/continual learning and ablations on embedding/window/features

Declarations

Conflict of interest

The authors declare no interest conflict. They have no known competing financial interests or personal relationships that could have appeared to influence the article reported in this article.

Author contribution

The contribution of each researcher in each of the points developed in this research were defined based on:

Medina-Martínez Sergio Iván: Conceptualization; Methodology; Software; Validation; Formal analysis; Writing original draft.

Juárez Toledo Carlos: Provided advice on the models and on the background for the state of the art. Supported the development of the method.

Carrillo-Martínez, Irma: Assisted in the data analysis and the assembly model and reviewed, corrected the article.

Hernández-Epigmenio, Miguel Angel: Manuscript review and feedback

Availability of data and materials

The datasets used in this study are publicly available from NASA's Li-ion Battery Aging Datasets

Funding

No internal or external funding was provided for this research project; however, it was made possible thanks to the postgraduate studies scholarship granted by la Secretaría de Ciencia, Humanidades, Tecnología e Innovación (SECIHTI).

Acknowledgements

To la Secretaría de Ciencia, Humanidades, Tecnología e Innovación (SECIHTI).

Abbreviations

AI	Artificial Intelligence
ALA	Artificial Lemming Algorithm
BMS	Battery Management System
CC	Constant Current
CNN	Convolutional Neural Network
CS	Cuckoo Search
CV	Constant Voltage
EOL	End-of-Life
EV	Electric Vehicle
FL	Federated Learning
GRU	Gated Recurrent Unit
IC	Incremental Capacity

Article

IE	Identity Embedding
IMF	Intrinsic Mode Function
LFP	Lithium Iron Phosphate (LiFePO ₄)
LIB	Lithium-Ion Battery
LSTM	Long Short-Term Memory
MAE	Mean Absolute Error
MAPE	Mean Absolute Percentage Error
NASA	NASA Prognostics Center of Excellence
PCoE	
NCA	Lithium Nickel Cobalt Aluminum Oxide (LiNiCoAlO ₂)
NCM	Lithium Nickel Cobalt Manganese Oxide (LiNiMnCoO ₂)
Pabs	Integrated Absolute Power (energy proxy)
PF	Particle Filter
RMSE	Root Mean Square Error
RNN	Recurrent Neural Network
Rproxy	Internal-Resistance Proxy
RUL	Remaining Useful Life
SA-LSTM	Self-Attention LSTM
SVR	Support Vector Regression
VMD	Variational Mode Decomposition
1D-CNN	One-Dimensional CNN

References

Antecedents

Luo, K., Chen, X., Zheng, H., & Shi, Z. (2022). A review of deep learning approach to predicting the state of health and state of charge of lithium-ion batteries. *Journal of Energy Chemistry*, 74, 159–173.

Medina-Martínez, S. I., Juárez-Toledo, C., & Martínez-Carrillo, I. (2024). Estimation of lithium-ion battery state of health using an ensemble model integrated with random forest and linear regression techniques. *Quantitative and Statistical Analysis*.

Ralls, A. M., Leong, K., Clayton, J., Fuelling, P., Mercer, C., Navarro, V., & Menezes, P. L. (2023). The Role of Lithium-Ion Batteries in the Growing Trend of Electric Vehicles. *Materials*, 16(17).

Shen, X., Liu, H., Cheng, X. B., Yan, C., & Huang, J. Q. (2018). Beyond lithium ion batteries: Higher energy density battery systems based on lithium metal anodes. *Energy Storage Materials*, 12, 161–175.

Tran, M. K., Panchal, S., Khang, T. D., Panchal, K., Fraser, R., & Fowler, M. (2022). Concept Review of a Cloud-Based Smart Battery Management System for Lithium-Ion Batteries: Feasibility, Logistics, and Functionality. *Batteries*, 8(2), 19.

Yang, S., Zhang, Z., Cao, R., Wang, M., Cheng, H., Zhang, L., Jiang, Y., Li, Y., Chen, B., Ling, H., Lian, Y., Wu, B., & Liu, X. (2021). Implementation for a cloud battery management system based on the CHAIN framework. *Energy and AI*, 5, 100088.

Basics

Ding, G., Wang, W., & Zhu, T. (2022). Remaining Useful Life Prediction for Lithium-Ion Batteries Based on CS-VMD and GRU. *IEEE Access*, 10, 89402–89413.

Saha, B., & Goebel, K. (2007). *Battery Data Set NASA Ames Research Center*.

Supports

Chen, B., Zhang, Y., Wu, J., Yuan, H., & Guo, F. (2025). Lithium-Ion Battery State of Health Estimation Based on Feature Reconstruction and Transformer-GRU Parallel Architecture. *Energies*, 18(5), 1236.

Cheng, S. (2025). A Hybrid Deep Learning Method for the Estimation of the State of Health of Lithium-Ion Batteries. *International Transactions on Electrical Energy Systems*, 2025(1), 2442893.

Peng, S., Sun, Y., Liu, D., Yu, Q., Kan, J., & Pecht, M. (2023). State of health estimation of lithium-ion batteries based on multi-health features extraction and improved long short-term memory neural network. *Energy*, 282, 128956.

Yu, Z., & Pan, Z. (2025). Joint Estimation of SOH and RUL for Lithium-ion Batteries using CNN-GRU Based on Artificial Lemming Algorithm. 1269–1274.

Differences

Alharbi, T., Umair, M., & Alharbi, A. (2025). Lithium-Ion Battery State of Health Degradation Prediction Using Deep Learning Approaches. *IEEE Access*, 13, 13464–13481.

Ravi, S., Koushik, P. G. V., Varma, V. C. K., & Rajeswari, S. (2022). [Li-ion Batteries SoH Estimation Using LSTM](#). *CSITSS 2022*.

Xu, H., Wu, L., Xiong, S., Li, W., Garg, A., & Gao, L. (2023). [An improved CNN-LSTM model-based state-of-health estimation approach for lithium-ion batteries](#). *Energy*, 276, 127585.

Discussions

Eleftheriadis, P., Gangi, M., Leva, S., Rey, A. V., Groppo, E., & Grande, L. (2024). [Comparative study of machine learning techniques for the state of health estimation of Li-Ion batteries](#). *Electric Power Systems Research*, 235, 110889.

Kong, X., Chen, Z., Liu, W., Ning, K., Zhang, L., Syauqie, ., Marier, M., Liu, Y., Chen, Y., & Feng Xia. (2025). [Deep learning for time series forecasting: a survey](#). *International Journal of Machine Learning and Cybernetics*, 16, 5079–5112.